

Temperature dependence of critical magnetic fields and electronic characteristics of Nb₃Ge films

A. I. Golovashkin, E. V. Pechen', and N. P. Shabanova

P. N. Lebedev Physics Institute, USSR Academy of Sciences

(Submitted 16 September 1981)

Zh. Eksp. Teor. Fiz. 82, 850-861 (March 1982)

The temperature dependences of the parallel and perpendicular critical magnetic fields were measured for Nb₃Ge films produced by cathode sputtering. An algorithm based on measurement of the derivative of the critical field in the region of the linear temperature dependence, of the resistivity, and of the conduction-electron density was used to determine the electronic characteristics, viz., the state density near the Fermi energy, the electron velocity on the Fermi surface, the area of the Fermi surface, the mean free path, and others, as well as superconducting-state parameters such as the depth of penetration of the field into the superconductor, the coherence length, the Ginzburg-Landau parameter, and the values of the critical magnetic field at $T = 0$. The observed dependence of the electronic characteristics on the electron mean free path is attributed to smearing of the abrupt singularities in the state density. The correlation between T_c and the area of the Fermi surface is obtained for superconductors with A15 lattice.

PACS numbers: 74.30.Ci, 74.70.Lp, 73.60.Ka, 71.20. + c

INTRODUCTION

Despite intensive investigations of the properties of the superconducting compound Nb₃Ge, the possibilities of raising its critical temperature T_c have not yet been fully exploited,¹ and a number of its principal electronic characteristics remain undetermined. It is important to ascertain how these characteristics vary as the A15 structure becomes ordered, and which of them exert the decisive influence on T_c .

Nb₃Ge comes closest to being stoichiometric in films having a composition C_0 whose value depends on the production conditions.¹ The phase that determines the T_c of the film has in this case likewise a composition close to C_0 .² In this study we determine the electronic characteristic of Nb₃Ge films with different values of C_0 , obtained in "soft" regimes, by measuring the temperature dependences of the critical magnetic field $H_{c2}(T)$. We have succeeded in tracking the variation of the characteristics as the sample comes close to having an ideal structure.

1. EXPERIMENT

The samples were prepared by cathode sputtering with direct current in an argon atmosphere using an ultrahigh vacuum facility. The partial pressure of the oxygen ranged from 10^{-5} to 3×10^{-7} Torr. The sputtering procedure is described in detail in Ref. 3. The value of T_c (which corresponds to the midpoint of the transition) was measured by a four-contact method accurate to 0.1 K. The temperature was measured with an Allen-Bradley thermometer. The resistivity measurement accuracy was 5-10% and was determined by the accuracy with which the film thickness d was measured. The superconducting-transition curves of the films were plotted at different values of the magnetic field, perpendicular (H_{\perp}) and parallel (H_{\parallel}) to the sample plane (the field was always perpendicular to the measurement current). The magnetic field, produced by a 165NS40H Intermagnetics (USA) superconducting solenoid and was measured accurate to within 0.1 kOe with a Hall pickup. The corrections

for the change of the thermometer readings in the magnetic field were obtained by using a standard capacitive thermometer made by the same firm. The beginning and end of the superconducting transitions were defined as the points at which the resistance deviated by 0.2%.

Figure 1 shows the temperature dependences of the perpendicular $H_{c2\perp}$ and parallel ($H_{c2\parallel}$) critical magnetic fields for three samples with different T_c . Some deviation of $H_{c2}(T)$ from linearity, in excess of the measurement error, was observed only in weak fields near T_c . The slopes in the linearity region of $H_{c2}(T)$ were $H'_{c2} \equiv -dH_{c2}/dT = 20$ to 26 kOe/K. In strong fields $H_{c2\perp}$ exceeds $H_{c2\parallel}$ noticeably. Near T_c (in weak fields), besides the deviation of $H_{c2}(T)$ from linearity, the ratio $H_{c2\perp}/H_{c2\parallel}$ decreases and apparently becomes less than unity in sample No. 119-z1.

Figures 2 and 3 show the temperature dependences of $H_{c2\perp}$ and $H_{c2\parallel}$ of sample 119-z1 at the start, mid-point, and end of the superconducting transition. A slight broadening of the superconducting transition, more pronounced in the case of H_{\perp} , is observed in strong fields. In weak fields, the transition is somewhat narrower than at $H = 0$. The deviation of H_{\parallel} from

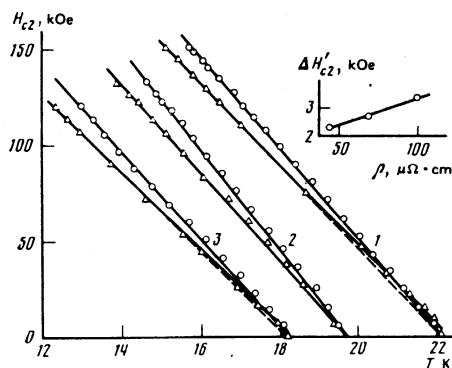


FIG. 1. Temperature dependences of perpendicular (circles) and parallel (triangles) critical magnetic fields for Nb₃Ge samples: 1) No. 119-z1, 2) No. 116-el, 3) No. 124-zh1. The inset shows the dependence of the change of the slope H'_{c2} on going from H_{\perp} to H_{\parallel} on the sample resistivity ρ .

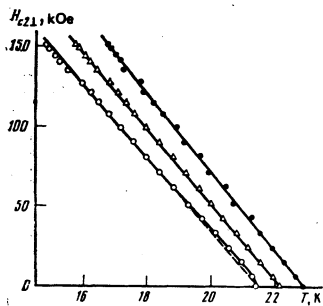


FIG. 2. Temperature dependence of critical field $H_{c2\perp}$ for sample 119-zl at the start (dark circles), midpoint (triangles), and end (light circles), of the superconducting transition.

linearity is more strongly pronounced near T_c . The $H_{c2}(T)$ curves plotted for the start of the transition are practically linear in the entire investigated field interval. The character of the plots in Figs. 2 and 3 indicates that they are determined by the main mass of the sample.

The higher critical fields obtained for films obtained by cathode sputtering in the case of H_{\perp} are attributed to their columnar structure.⁴ A particularly distinct granular structure was observed by us in films produced in "hard" regimes.⁵ Improvement of the film structure (decrease of the resistivity) leads to a decrease in the difference between the slopes $H'_{c2\perp}$ and $H'_{c2\parallel}$, as seen from Fig. 1. In the calculation of the electronic characteristics it is customary to use the quantity

$$H_{c2}' = -(dH_{c2}/dT)_{T=T_c}$$

obtained in a perpendicular field. In samples with $H_{c2\perp} > H_{c2\parallel}$, however, the closest to the upper critical field H_{c2} is $H_{c2\parallel}$. In addition, the presence near T_c of effects due to the change of the relation between the roughness size, grain size, and film thickness, on the one hand, and the Ginzburg-Landau coherence length $\xi_{GL}(T)$ on the other, the values of H'_{c2} for the linearity region of $H_{c2}(T)$ must be used in the calculation of the electronic characteristics.

In a real film having a columnar structure, a superconducting contact exists not between all neighboring columns. A somewhat idealized conception is that an intricate network of intersecting cylindrical superconducting regions, perpendicular to the substrate, is produced in the film. The characteristic thickness of

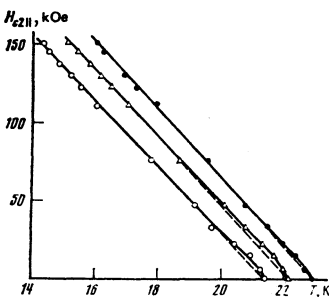


FIG. 3. Temperature dependence of $H_{c2\parallel}$ for sample 119-zl. The notation is the same as in Fig. 2.

these regions is determined by the diameter of the columns. The magnetic field, which is perpendicular to the plane of the sample, turns out to be parallel to the surfaces of these superconducting regions. It is this which causes the critical field $H_{c2\perp}$ to be stronger than $H_{c2\parallel}$. Contributing to this effect, to one degree or another, is the increase of the upper critical field as a result of both surface conductivity ($H_{c3} \approx 1.69H_{c2}$) for an ideal surface and the "total" penetration of the field (in this case the critical field is $2\sqrt{3}H_{c2}\xi_{GL}/L$). The dimension L is determined by the diameter of the columns. The near-spherical form of the upper surfaces of the columns leads practically to absence of the effect of surface conductivity far from T_c in the case of a field H_{\parallel} . In this case there is likewise no size effect, because of the large film thickness.

As the sample temperature approaches T_c , the value of ξ_{GL} increases and at $\xi_{GL} \gg L$ the surface superconductivity manifests itself in full strength in the case of H_{\parallel} .

The experimental values of the parameters of the investigated films are given in the upper part of Table I, together with the parameters of the "amorphous" parameters of the sample of Ref. 6, obtained by evaporation in vacuum and bombarded by 2.5-MeV α particles. In the table, ρ is the resistivity at $T = 25$ K, ρ_r/ρ is the ratio of the resistivities at room temperature and 25 K, $H'_{c2\parallel}$ and $H'_{c2\perp}$ are respectively the values of H'_{c2} for H_{\parallel} and H_{\perp} . We note that ρ still does not coincide with the residual resistivity, inasmuch as ρ depends on T at fields stronger than critical.

It must be constantly kept in mind that in the calculation of the electronic characteristics one must use the value of ρ of precisely that part of the A15 phase which

TABLE I.

Characteristics	Sample No.			
	119-zl	124-zh1	116-et	"Amorphous"
Experiment				
T_c , K	22.1	18.2	19.7	4
ρ , $\mu\Omega \cdot \text{cm}$	44.5	68.5	100	150
ρ_r/ρ	2.2	1.6	1.7	-
d_r , μ	0.40	0.42	0.7	-
$H'_{c2\parallel}$, kOe/K	21.6	20.4	23.1	-
$H'_{c2\perp}$, kOe/K	23.9	23.1	26.4	18
Calculation				
λ	1.8	1.55	1.65	0.7
γ^* , mJ/cm ² K ²	0.57	0.46	0.38	0.3
$N^*(0)$, st/eV · at · spin	1.23	1.00	0.83	0.6
$N^*(0)/N_0(0)$	5.4	4.4	3.7	3
$N(0)$, st/eV · at · spin	0.44	0.39	0.31	0.3
S	0.21	0.21	0.21	0.4
N , 10 ²² cm ⁻³	0.65	0.73	0.91	3
v_F^* , 10 ⁷ cm/sec	0.92	1.1	1.4	4
v_F , 10 ⁷ cm/sec	2.6	2.9	3.6	6
λ_{tr}	1.6	3.7	6.0	300
l , Å	32	21	14	5
D^* , cm ² /sec	0.97	0.78	0.64	0.6
ξ_0^* , Å	57	86	95	1000
ξ_{GL}^0 , Å	26	30	27	70
λ_L , Å	1100	990	900	400
λ_{GL}^0 , Å	890	1100	1200	4000
κ	34	38	46	60
ω_0 , meV	14.2	13.4	13.7	10
$H_c(0)$, kOe	4.4	3.2	3.2	0.5
$H_{c1}(0)$, kOe	330	260	320	50

*The experimental data for this sample were taken from Ref. 6.

is responsible for T_c . The actually measured ρ can differ noticeably (is usually higher) in the case of inhomogeneously samples, particularly those with more than one phase. In our case, thus, the most homogeneous sample was No. 119-z1. The value of ρ for the high-temperature phase of sample No. 116-e1 is apparently somewhat lower than that actually measured, since the sample was prepared in a relatively harder regime. Nonetheless, the x-ray results and the small broadening of the superconducting transition of the sample in strong fields, compared with $H=0$, indicates that its deviation from single-phase is small.

2. ALGORITHM FOR THE CALCULATION OF THE CHARACTERISTICS

To calculate the electronic characteristics of the Nb_3Ge films we used an algorithm based on the Ginzburg-Landau theory for type-II superconductors, with corrections for the strong coupling. A number of relations needed for the calculations were used in the form given in Ref. 7. The calculations were based on expressions that take into account the ratio of the electron mean free path l and the coherence length ξ^* (Ref. 8).

The connection between $H'_{c2} = \hbar c / 2e (\xi_{GL}^0)^2 T_c$ and the electronic characteristics can be written in the form⁷

$$H'_{c2} = \frac{\eta_{Hc2}(T_c)}{R(\lambda_{tr})} \left[\frac{24}{7\zeta(3)} \left(\frac{3}{\pi} \right)^{1/2} \frac{\hbar c}{k^2 e} T_c \frac{\gamma^*}{N_{val}^{1/2} S^2} + \frac{12}{7\pi\zeta(3)} \frac{ec}{k} \frac{\rho\gamma^*}{9 \cdot 10^{11}} \right] N^*(0) \quad (1)$$

or

$$H'_{c2} = \frac{\eta_{Hc2}(T_c)}{R(\lambda_{tr})} \left[\frac{16\pi^2}{7\zeta(3)} \frac{cmk^2}{eh} \frac{T_c}{N} (1 - \lambda) + \frac{8\pi}{7\zeta(3)} eck \frac{\rho}{9 \cdot 10^{11}} \right] N^*(0). \quad (2)$$

Here $\zeta(3) \approx 1.202$, k is Boltzmann's constant, c is the speed of light, \hbar is Planck's constant, e and m are the charge and mass of the free electron, λ is the electron-phonon interaction constant, η_X reflects the additional strong-coupling correction for the quantity X (Ref. 9), N_{val} is the density of the valence electrons, γ^* is the renormalized coefficient of the electronic part of the heat capacity, S is the ratio of the area of the Fermi surface to the area of the Fermi sphere of the free electrons at a density N_{val} , N is the unrenormalized (optical) density of the conduction electrons, $N^*(0) = N(0)(1 + \lambda)$ is the renormalized density of the electronic states near the Fermi energy, $N(0)$ is the "band" density of the electronic states, the coefficient $R(\lambda_{tr})$ is of the order of unity ($R(0) = 1$, $R(\infty) = \pi^2 [7\zeta(3)]^{-1} \approx 1.173$), $\lambda_{tr} = \pi e^{-\gamma} \xi_0^*/2l \approx 0.882 \xi_0^*/l$, and $e^{-\gamma} \approx 1.781$ (Ref. 8). The resistivity ρ in (1) is in Ω -cm. On going from (1) to (2), the relations used were

$$\gamma^* = 2\pi^2 k^2 N^*(0)/3, \quad (3)$$

$$S = (N/N_{val})^{1/2} (N(0)/N_c(0))^{1/2}, \quad (4)$$

where the density of the free electrons per spin is

$$N_c(0) = \frac{1}{2\pi} \left(\frac{3}{\pi} \right)^{1/2} \frac{m}{\hbar^2} N_{val}^{1/2} = 1.28 \cdot 10^{26} N_{val}^{1/2}. \quad (5)$$

Equation (4) was obtained in Ref. 10, and in the derivation of (2) and (4) we used an approach in which the

change of N/m on account of the nonsphericity of the Fermi surface is related to the electron density and not to their mass.

The state density can thus be directly determined from (2) if N is known,

$$N^*(0) = H'_{c2} \eta_{Hc2}^{-1} (T_c) R(\lambda_{tr}) [1.93 \cdot 10^{-11} T_c N^{-1} (1 + \lambda) + 6.60 \cdot 10^{-17} \rho]^{-1} \quad (6)$$

or from (1) and (3) if data on S are available,

$$N^*(0) = -2.20 \cdot 10^{16} (N_{val}^{1/2} S)^2 \rho T_c^{-1} + \{ [2.20 \cdot 10^{16} (N_{val}^{1/2} S)^2 \rho T_c^{-1}]^2 + 6.66 \cdot 10^{26} H'_{c2} \eta_{Hc2}^{-1} (T_c) R(\lambda_{tr}) \eta_{Hc2}^{-1} (T_c) T_c^{-1} \}^{1/2}. \quad (7)$$

The mean electron velocity on the Fermi surface is $v_F^* = v_F / (1 + \lambda)$, where v_F is the band value of the velocity, and can be obtained from one of the equations

$$v_F^* = \left(\frac{3N}{2mN(0)} \right)^{1/2} \frac{1}{1 + \lambda} = v_{F0} \left(\frac{N}{N_{val}} \right)^{1/2} \left(\frac{N_c(0)}{N(0)} \right)^{1/2} \frac{1}{1 + \lambda}. \quad (8)$$

Here v_{F0} is the electron velocity for the Fermi sphere at a density N_{val} . The coherence length is

$$\xi_0^* = \frac{\hbar v_F^*}{\pi^2 e^{-\gamma} k T_c} = 1.38 \cdot 10^{-12} \frac{v_F^*}{T_c}. \quad (9)$$

The Ginzburg-Landau coherence length is

$$\xi_{GL}(T) = [\hbar c / 2e H_{c2}(T)]^{1/2} = [\hbar c / 2e H_{c2}(T_c - T)]^{1/2} = \xi_{GL}^0 / (1 - T/T_c)^{1/2}, \quad (10)$$

$$\xi_{GL}^0 = 1.81 \cdot 10^{-4} / (T_c H_{c2})^{1/2}.$$

The depth of penetration of the magnetic field into the superconductor is

$$\lambda_{GL}(T) = \frac{\eta_{\lambda}(T_c) \lambda_{BGS}(0)}{2^{1/2} (1 - T/T_c)^{1/2}} = \frac{\lambda_{GL}^0}{(1 - T/T_c)^{1/2}}, \quad (11)$$

where $\lambda_{BGS}(0)$ is the penetration depth in accord with the weak-coupling theory.

The London penetration depth is

$$\lambda_L = \frac{(9\pi)^{1/2} \hbar c \sqrt{\gamma^*}}{2\pi k e N_{val}^{1/2} S} = 1.32 \cdot 10^8 \frac{\sqrt{\gamma^*}}{N_{val}^{1/2} S}. \quad (12)$$

The diffusion coefficient is

$$D = v_F^* l / 3 = 9 \cdot 10^{11} [2e^2 N^*(0) \rho]^{-1}. \quad (13)$$

Characteristics such as the mean free path l , the Ginzburg-Landau parameter κ , the heat-capacity discontinuity at $T = T_c$, the parameter λ_{GL}^0 , and the quantity $H'_c \equiv -(dH_c/dT)_{T=T_c}$ can be obtained from the values of ρ , S , N_{val} , and γ^* by using the expressions of Ref. 7.

The thermodynamic critical magnetic field near T_c is

$$H_c(T) = \left(\frac{8}{7\zeta(3)} \right)^{1/2} e^{\gamma} \frac{\eta_{Hc}(T_c)}{\eta_{Hc}(0)} H_c(0) \left(1 - \frac{T}{T_c} \right) = 1.74 \frac{\eta_{Hc}(T_c)}{\eta_{Hc}(0)} H_c(0) \left(1 - \frac{T}{T_c} \right), \quad (14)$$

where the critical field at $T = 0$ is

$$H_c(0) = \sqrt{6\pi} e^{-\gamma} \eta_{Hc}(0) T_c \sqrt{\gamma^*} = 2.44 \eta_{Hc}(0) T_c \sqrt{\gamma^*}. \quad (15)$$

The equation for the upper critical field in the "dirty" limit without allowance for the paramagnetic restriction on the spin-orbit scattering was obtained in Ref. 11. As $T \rightarrow T_c$, with allowance for the strong-coupling corrections,

$$H_{c2}(T) = \frac{8e^v}{\pi^2} H_{c2}(0) \left(1 - \frac{T}{T_c}\right) \frac{\eta_{H_{c2}}(T_c)}{\eta_{H_{c2}}(0)}. \quad (16)$$

Hence

$$H_{c2}(0) = \frac{\pi^2}{8e^v} T_c H_{c2}' \frac{\eta_{H_{c2}}(0)}{\eta_{H_{c2}}(T_c)} = 0.693 T_c H_{c2}' \frac{\eta_{H_{c2}}(0)}{\eta_{H_{c2}}(T_c)}. \quad (17)$$

The value of $H_{c2}(0)$ can be expressed in this case also in terms of other physical characteristics:

$$H_{c2}(0) = \sqrt{2} \frac{\pi^2 \kappa(T_c)}{2(14\xi(3))^{1/2}} H_c(0) \frac{\eta_{H_{c2}}(0)}{\eta_{H_c}(T_c) \eta_{H_{c2}}(0)}. \quad (18)$$

In the "pure" limit we have¹¹

$$H_{c2}(0) = 0.74 T_c H_{c2}' \frac{\eta_{H_{c2}}(0)}{\eta_{H_{c2}}(T_c)}. \quad (19)$$

The upper critical field at $T=0$, which is bounded by the paramagnetic limit (without allowance for spin-orbit scattering), can be obtained from the equation¹²

$$H_{c2}'(0) = H_{c2}(0) (1 + \alpha^2)^{-1/2}, \quad (20)$$

where $\alpha = \sqrt{2} H_{c2}(0) / H_p(0)$ is the Maki parameter,⁷ and

$$H_p(0) = \sqrt{2} \pi e^{-v} \frac{kmc}{\hbar} (1 + \lambda)^{1/2} T_c \eta_{H_c}(0) = 1.86 \cdot 10^4 \eta_{H_c}(0) (1 + \lambda)^{1/2} T_c. \quad (21)$$

is the limiting Pauli field.

Allowance for the spin-orbit interaction, which is characterized by the constant λ_{so} , decreases the role of the paramagnetic restriction.¹³ At $\lambda_{so} \gg 1$ the effective limiting field is¹⁴

$$H_{so} \approx 1.33 \lambda_{so}^{1/2} H_p(0). \quad (22)$$

so that in the limit of an infinite spin-orbit interaction the paramagnetic restriction on $H_{c2}(0)$ is completely lifted.

The strong-coupling correction for the energy gap Δ is^{15,16}

$$\eta_{\Delta}(0) = \frac{\Delta}{\pi e^{-v} k T_c} = 0.567 \frac{\Delta}{k T_c} = 1 + 5.3 \left(\frac{T_c}{\omega_0}\right)^2 \ln \frac{\omega_0}{T_c}, \quad (23)$$

where ω_0 is the characteristic frequency of the phonon spectrum, and makes it possible to determine the ratio T_c/ω_0 from the value of Δ . This ratio permits calculation of the η_{χ} correction for other quantities, such as, H_{c2} , ξ_{GL} , λ_{GL} , H_c , and κ , using the equations of Ref. 17.

3. ELECTRONIC CHARACTERISTICS

The algorithm described in the preceding section makes it possible in principle to determine a large number of electronic characteristics by measuring the temperature dependence of the critical magnetic field and the resistivity of the sample. Besides these quantities, one must know the area of the Fermi surface⁷ or the density of the conduction electrons. If the density $N^*(0)$ of the electronic states on the Fermi surface is known from measurements of the heat capacity, the algorithm can be used also to determine N and S .

It should be noted that those terms in the expressions for H_{c2}' that contain N and S are relatively large only when the pure limit is approached. Since the inter-

mediate case is usually realized in materials with A15 lattice, which is close to the dirty limit, the influence of the possible inaccuracy in the determination of N and S on the determination of the other characteristics is weakened to the extent that the first term in (1) and (2) is small.

The electronic characteristics of the investigated Nb₃Ge samples, determined using the algorithm described above, are listed in the table, which contains for comparison the characteristics of an "amorphous" sample, estimated on the basis of the data of Ref. 6. We have $N_{val} = 28.0 \cdot 10^{22} \text{ cm}^{-3}$. For the sample with the maximum T_c we used the values $N = 0.65 \cdot 10^{22} \text{ cm}^{-3}$ (Ref. 18) and $2\Delta/kT_c = 4.2$ (Refs. 19 and 20). From the calculated value of ω_0 we can determine the ratio ω_0/Θ , where Θ is the Debye temperature. Despite the relatively small difference between the values of Θ in the crystalline and amorphous samples (302 and 222 K, Ref. 21), a linear correction for its variation with T_c was introduced. The values of ω_0 obtained in this manner make it possible to calculate η_{χ} and λ . The values of λ were calculated from the McMillan formula and agree satisfactorily with the values obtained from the Eliashberg equation using the Einstein spectrum and with the curve of Allen and Dynes drawn through the experimental data (Ref. 22).

The value of S was calculated for the sample No. 119-z1. The same value was assumed for samples 124-zh1 and 116-e1; this is a sufficiently good approximation, since the lattice constant does not change greatly in the range of variation of T_c of the investigated samples, and the effects of "smearing" of the Fermi surface, due to the small mean free path, are significant in practice only for the amorphous sample. For the latter, S was estimated from the value $l \approx 5 \text{ \AA}$ cited in Ref. 6.

The field $H_{c2}(0)$ was calculated without allowance for the paramagnetic restriction under the assumption that $\eta_{H_{c2}}(0) = \eta_{H_{c2}}(T_c)$. The critical magnetic fields for sample No. 119-z1 in parallel and perpendicular fields, determined for the start of the transition, are respectively $H_{c2\parallel}(0) = 350$, $H_{c2\perp}(0) = 390$. Experiment²³ yielded $H_{c2\perp}(4.2 \text{ K}) = 370 \text{ K}$ for a similar Nb₃Ge sample, in good agreement with our data. It is shown in Ref. 23 that there is no paramagnetic restriction for the investigated Nb₃Ge films, i.e., the value of λ_{so} is large. In our case $H_p(0) = 770 \text{ kOe}$ so that assuming that the suppression of the field $H_{c2}(0)$ does not exceed 10 kOe we obtain $\lambda_{so} \approx 5$. This leads to a characteristic spin-orbit scattering length of the order of 10 Å, noticeably less than the value of l . One possible cause of this discrepancy is failure to allow for the temperature dependence of the correction $\eta_{H_{c2}}$.

4. DISCUSSION

The described algorithm makes it possible, by measuring a few physical characteristics, to obtain a large number of the most important parameters of a strong-coupling superconductor, both for the normal and for the superconducting state of the material. To estimate

the accuracy of the algorithm and the validity the assumption made in it, it is very important to compare the results with data from other experiments. In Ref. 7 are analyzed data obtained for Nb₃Sn and V₃Si by using a similar algorithm based on a fit to the area of the Fermi surface. The authors of that reference have shown that it is possible to reconcile their results with the coefficient obtained for the linear heat-capacity term γ^* obtained from the temperature dependence of the heat capacity.

A number of papers^{6,24,25} cite values of γ^* determined experimentally by measuring the heat capacity. The value of γ^* is approximately 0.3 (Refs. 6 and 24) or (0.37 ± 0.01) mJ/cm³ · K² (Ref. 25). These are close to the 0.28 mJ/cm³ · K² obtained by us for a sample with $T_c = 19.7$ K and $\rho \approx 100$ $\mu\Omega \cdot \text{cm}$. Magnetic measurements⁵ yielded $\gamma^* = 0.34$ mJ/cm³ · K² for a sample with $T_c \approx 20$ K. According to heat-capacity measurements, the decrease of the state density $N(0)$ on going from an Nb₃Ge sample with $T_c \approx 21$ K to an amorphous sample with $T_c \approx 4$ K is ~50%,⁸ in good agreement with our data. We note there are no fit parameters in the algorithm used by us.

It is of interest to examine the changes of the obtained electronic characteristics when certain sample parameters are changed. The dependences of various characteristics of the investigated sample on the electron mean free path are shown in Fig. 4. The data of Table I and Fig. 4 show a significant change in the electronic characteristics with decreasing mean free path l . (Since the composition change is $\Delta C_0 \leq 1\%$, the ensuing change in the characteristics is negligibly small.) The "smearing" of the Fermi energy E_F and of other characteristics should be observed when the energy uncertainty is

$$\Delta E_F \approx \hbar/\tau = \hbar v_F/l \sim E_F,$$

i.e., at (for free electrons)

$$l \sim a / [(3\pi^2/8)zn_0]^{1/3}.$$

Here τ is the electron relaxation time, z is the valence, and n_0 is the number of atoms in the unit cell.

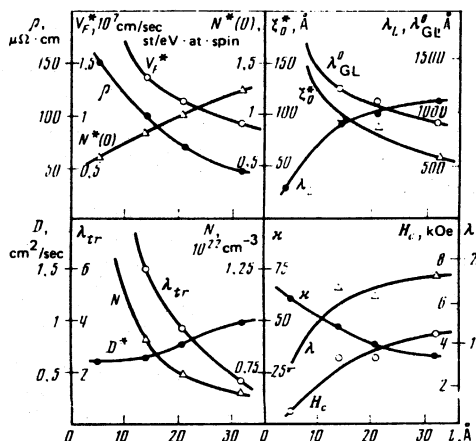


FIG. 4. Electronic characteristics and parameters of Nb₃Ge films vs mean free path l .

Even if we allow that actually v_F is much less than its value for free electrons, radical changes should be expected at $l \leq a$. The changes observed in experiment at larger values of l are due to the effect of the relaxation time on the smearing of the abrupt singularities in the state density.⁶

The observed dependence on l (or, equivalently, on ρ) of such characteristics as $N(0)$, N , v_F , and λ should cause them to be temperature-dependent. This dependence can be obtained on the basis of Fig. 4 if the dependence of l (or ρ) on T is known from experiment. It is seen, for example, that for sample No. 119-z1 ($\rho_r/\rho = 2.2$) a change from 25 K to room temperature should increase N by 40% and decrease $N^*(0)$ by 50%. Even more noticeable changes of the electronic characteristics should be expected with further rise in temperature (as $l \rightarrow a$). The noted dependence of the characteristics on T is due to the fact that l reaches low values sufficient to smear out the abrupt state-density singularities. In high-temperature superconductors with A-15 lattice the value of l is affected by the ordinary electron-factor scattering, by the Debye-Waller factor,²⁶ as well as by scattering from impurities and defects. The strong dependence of the indicated characteristics on T is due to the strong electron-phonon interaction in such superconductors. The smearing of the singularities of the electronic spectrum in these superconductors at sufficiently high temperature ($T \gg T_c$) is given by

$$\Delta E \approx 2\pi k(\lambda_{tr} T_c + \lambda T).$$

The first term determines here the smearing due to scattering from impurities and defects (λ_{tr} corresponds to a temperature 25 K, and the quantity of the electron-phonon interaction to this quantity is neglected). At $T \approx T_c$ the smearing $\Delta E \approx 2\pi k\lambda_{tr} T_c$ amounts to ~0.02 eV even in a sample with $T_c = 22$ K.

The limiting value of the resistivity ρ with decreasing l can be estimated. Assuming that at the limit $l = l_{lim} \sim a/2 - a$, we obtain

$$\rho_{lim} = \frac{3}{2e^2} 9 \cdot 10^{11} \frac{1}{v_F N(0)} \frac{1}{l_{lim}} \sim 200-300 \mu\Omega \cdot \text{cm}.$$

This estimate shows that the limiting values of ρ and of other characteristics have not yet been reached in the amorphous sample.

It is seen from Fig. 4 that many characteristics have not reached values corresponding to a fully ordered stoichiometric sample even in the best sample. For a sufficiently good approach to an "ideal" sample a value $l \sim 60$ Å must be reached (in the β phase of a composition close to stoichiometric). It follows from the dependence of N on l (Fig. 4) that $N \approx 0.5 \times 10^{22}$ cm⁻³ in ideal Nb₃Ge. A limiting value $T_c = 27$ to 30 K was previously estimated¹ for stoichiometric Nb₃Ge with maximum order. Figure 5 shows the dependence of T_c on N for high-temperature superconductors with A15 lattice.²⁷ The hypothetical ideal Nb₃Ge likewise agrees well with this dependence. It is seen from the figure that critical temperatures noticeably above 30 K are difficult to achieve, for this calls for the production of samples with very low conduction-electron

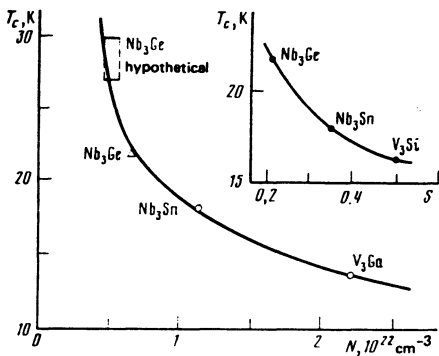


FIG. 5. Dependence of T_c on N for superconductors with A15 lattice. The inset shows the dependence of T_c on S for such materials.

density (the semiconducting "break"). Figure 5 shows only the data for materials with A15 lattice that are closest to stoichiometric. The tendency shown (the lowering of T_c with increasing N or N/N_{val}) is preserved if known data are added for all metals and alloys, including some with nonoptimal composition.²⁷ This general dependence is confirmed also by the amorphous sample,⁶ the value of N for which is estimated in the present article. It must be recognized that such samples begin to be influenced not only by the smearing of the abrupt state-density singularities, but to a considerable degree also by the loss of crystal symmetry. The inset of Fig. 5 shows the dependence of T_c on the ratio of the area of the Fermi surface to the area S of the free-electron sphere for three superconductors with A15 lattice. The values of S for Nb_3Sn and V_3Si were obtained in Ref. 7, and for Nb_3Ge in the present study. The observed dependence agrees with other correlations of T_c and of the electronic characteristics.²⁷

The results attest to an increase of $H_{c2}(0)$ with T_c . If the linear character of this dependence is extrapolated, one can expect for samples with $T_c = 27$ to 30 K values $H_{c2}(0) \approx 400$ to 450 kOe (at the midpoint of the transition). It must be noted that we made no attempt to optimize the sample preparation conditions for the purpose of obtaining maximum values of H_{c2} . One can expect, in particular, samples having a specified T_c and obtained in the hard regime (dirtier) to have higher values of H_{c2} . A definite increase of H_{c2} can be reached at a certain deviation from the C_0 composition, owing to the influence of the parasitic phases on the value of ρ of the A15 phase.

The investigations of the properties of superconductors with A15 lattice indicate that they are highly interesting physical objects. We have in mind here not only their unusually high values of T_c and tremendous H_{c2} . At sufficiently small values of l these materials can be sufficiently pure superconductors in the sense that the ratio ξ^*/l is small ($\xi^*/l < 1.8$ in the sample with the maximum T_c). They have in this

case very high values of κ , reaching 30–50. At the same time, the smallness of the electron mean free path leads already to dependences of $N(0)$, N , v_F , and λ on l , which should naturally be reflected in their superconducting properties.

In conclusions, the authors thank V. I. Tsebro, V. M. Zakosarenko, and Yu. F. El'tsev for help with the work and for a discussion of the results.

- ¹A. I. Golovashkin, N. P. Kokoeva, and E. V. Pechen', *Kratk. Soobshch. Fiz.* No. 12, 32 (1980).
- ²A. I. Golovashkin, E. V. Pechen', A. I. Skvortsov, and N. E. Khlebova, *Fiz. Tverd. Tela (Leningrad)* **23**, 1324 (1981) [*Sov. Phys. Solid State* **23**, 774 (1981)].
- ³H. F. Braun, E. N. Haeussler, and E. J. Saur, *IEEE Trans. Magnetics*, **MAG-13**, 327 (1977).
- ⁴A. I. Golovashkin and E. V. Pechen', *Pis'ma Zh. Eksp. Teor. Fiz.* **30**, 561 (1979) [*JETP Lett.* **30**, 529 (1979)].
- ⁵H. Wiesmann, M. Gurvich, A. K. Ghosh, H. Lutz, O. F. Kammerer, and M. Strongin, *Phys. Rev.* **B17**, 122 (1978).
- ⁶T. P. Orlando, E. J. McNiff, Jr., S. Foner, and M. R. Beasley, *Phys. Rev.* **B19**, 4545 (1979).
- ⁷N. R. Werthamer, in: *Superconductivity*, R. E. Parks, ed., Dekker, 1969, Vol. 2, p. 321.
- ⁸D. Rainer and G. J. Bergmann, *Low Temp. Phys.* **14**, 501 (1974).
- ⁹A. I. Golovashkin and A. L. Shelekhov, *FIAN Preprint No.* 96, 1981.
- ¹⁰E. Helfand and N. R. Werthamer, *Phys. Rev.* **147**, 288 (1966).
- ¹¹K. Maki, *Physics* **1**, 124 (1964).
- ¹²N. R. Werthamer, E. Helfand, and P. C. Hohenberg, *Phys. Rev.* **147**, 295 (1966).
- ¹³P. Fulde and K. Maki, *Phys. Rev.*, **141**, 275 (1966). O. Fisher, *Helv. Phys. Acta* **45**, 331 (1972).
- ¹⁴B. T. Geilikman and V. Z. Kresin, *Fiz. Tverd. Tela (Leningrad)* **7**, 3294 (1965) [*Sov. Phys. Solid State* **7**, 2659 (1966)].
- ¹⁵D. F. Moore, R. B. Zubeck, J. M. Rowell, and M. R. Beasley, *Phys. Rev.* **B20**, 2721 (1979).
- ¹⁶N. F. Masharov, *Fiz. Tverd. Tela (Leningrad)* **16**, 2342 (1974) [*Sov. Phys. Solid State* **16**, 1524 (1975)].
- ¹⁷W. W. Yao, Ph. D. Thesis, Princeton Univ., 1978. L. F. Mattheiss, L. R. Testard, and W. W. Yao, *Phys. Rev.* **B17**, 4640 (1978).
- ¹⁸J. M. Rowell and P. H. Schmidt, *Appl. Phys. Lett.* **29**, 622 (1976).
- ¹⁹C. C. Tsuei, W. L. Johnson, R. B. Laibowitz, and J. M. Viggiano, *Sol. St. Commun.* **24**, 615 (1977).
- ²⁰C. C. Tsuei, S. Von Molnar, and J. M. Coey, *Phys. Rev. Lett.* **41**, 664 (1978).
- ²¹P. B. Allen and R. C. Dynes, *Phys. Rev.* **B12**, 905 (1975).
- ²²S. Foner, E. J. McNiff, Jr., J. R. Gavaler, and M. A. Janocko, *Phys. Lett.* **47A**, 485 (1974).
- ²³J. M. E. Harper, T. H. Geballe, L. R. Newkirk, and F. A. Valencia, *J. Less Comm. Metals* **43**, 5 (1975).
- ²⁴G. R. Stewart, L. R. Newkirk, and F. A. Valencia, *Sol. St. Commun.* **26**, 417 (1978).
- ²⁵G. P. Motulevich, *Zh. Eksp. Teor. Fiz.* **51**, 1918 (1966) [*Sov. Phys. JETP* **24**, 1287 (1966)]. A. E. Karakozov and E. G. Maksimov, *Sol. St. Commun.* **33**, 929 (1980).
- ²⁶A. I. Golovashkin and T. A. Kuznetsova, *FIAN Preprint No.* 170, 1980.

Translated by J. G. Adashko